

# Restoration of a Poissonian-Gaussian color moving-image sequence

Takahiro Saito<sup>1</sup>, Takashi Komatsu<sup>1</sup>

<sup>1</sup> Department of Electrical, Electronics & Information Engineering, Kanagawa University  
3-27-1 Rokkakubashi, Kanagawa-ku, Yokohama, 221-8686 Japan  
E-mail: {saitot01, komatt01}@kanagawa-u.ac.jp

**Abstract** An image taken under an extremely-low-illumination condition is modeled as obeying the Poissonian-Gaussian probability distribution. This paper presents our recently proposed image-restoration method to recover a higher-quality color moving-image sequence from those Poissonian-Gaussian random observations. The method firstly performs virtual multiplex imaging, formed as a series of pixel binning and redundant subsampling, on the input sequence for increasing its statistical reliability, secondly denoises the multiple subsampled image sequences given by the redundant subsampling, and lastly removes image blurs due to the pixel binning by super-resolution deblurring, which integrates the multiple denoised image sequences into an image sequence with the spatiotemporal resolution identical to that of the input image sequence. Through computer simulations, this paper demonstrates that the method successfully recovers a relatively-high-quality image sequence.

**Keywords:** pixel binning, redundant subsampling, denoising, super-resolution deblurring

## 1. Introduction

Recently, as a candidate successor to a CMOS image sensor, a quanta image sensor (QIS) attracts researchers' attention [1] ~ [6]. The QIS is expected to have single photon sensitivity [2] and to render its pitch size very small, e.g. 500nm [3], and hence the QIS is regarded as having the potential to achieve high spatial resolution, a high dynamic range, and so on. However, since a full well capacity of the QIS is generally set extremely small, a pixel's signal value observed by the QIS should be treated as a binary random variable. The observed signal of the QIS is statistically modeled as a two-level quantization output of a Poisson random process, that is to say, the output will be 1 if the photon count is over a certain threshold, and the output is 0 if the count is under the threshold. Therefore, to utilize the QIS as an image sensor instead of a CMOS image sensor, a highly-advanced image-restoration algorithm is indispensable, that is to say, an image sequence with desirable spatiotemporal resolution and/or a specifically satisfactory dynamic range should be restored from those seemingly uninformative binary quantized Poisson random process. From this point of view, recently preliminary studies on the issue of the QIS image restoration has been performed and some image restoration methods based on the statistical model of the binary quantized Poisson random process have been presented [4], [5], [6].

On the other hand, if a highly-advanced image-restoration algorithm is applied to a pixel's signal value observed by a CMOS image sensor, naturally the potential of the CMOS image sensor will be further extended. Along this line, recently, some researchers have been involved in the development of an image restoration method to heighten the potential for low-illumination photographing [7] ~ [17]. This paper takes up this issue, and presents our recently proposed image restoration method [17].

In the situation of extremely-low-illumination photographing such as video surveillance operating in the dark, a quantity of light incident on an image sensor is too small to utilize an image acquired by the image sensor, as it is, because of its very low picture-quality. Under such an extremely-low-illumination condition, a photoelectric conversion signal acquired by the sensor shows a statistical property of the Poisson distribution, and hence recently some researchers have developed image-processing methods to recover an image with relatively high picture-quality from an input Poissonian image whose pixel's

value obeys a Poisson distribution [7] ~ [12]. However, the Poisson distribution is insufficient to model a statistical property of real signals acquired by the sensor under the extremely-low-illumination condition, and actually random noise due to electronic circuits installed in the sensor, viz. read-out noise, is added to the real signals. The random noise is approximately modeled as obeying a white Gaussian distribution, and hence as the statistical model for the extremely-low-illumination image the Poissonian-Gaussian statistical model that a white Gaussian random number is added to a Poisson random number is regarded as far preferable to the Poisson statistical model.

As for the restoration of an input image obeying the Poissonian-Gaussian statistical model [13] ~ [17], Mäkitalo and Foi have recently proposed an image restoration method that firstly applies to an input image the generalized Anscombe transform, behaving as the variance stabilization transform for the Poissonian-Gaussian statistical model, then applies the existing state-of-the-art image-denoising method, e.g. the BM3D method [18], and finally applies the exact unbiased inverse of the generalized Anscombe transform [14]. Moreover, very recently, Chouzenoux and others have proposed a convex-optimization image-restoration approach with the exact Poissonian-Gaussian negative log-likelihood [16]. In the case of the extremely-low-illumination condition where total noise's power competes with signal's power almost equally, statistical reliability of a Poissonian-Gaussian random variable is so low that these recently-proposed approaches do not necessarily perform as well as expected, and hence a certain approach to heighten the signal-to-noise power ratio should be incorporated into the restoration process at any risk.

From the above-mentioned point of view, we have tackled an image-restoration problem that recovers a color moving-image sequence with higher picture-quality from a Poissonian-Gaussian image sequence, and very recently we have proposed a new concept that both virtual multiplex imaging, constructed as a series of spatiotemporal pixel-binning and 3-D redundant subsampling, and super-resolution deblurring are simultaneously introduced into the restoration approach [17].

## 2. Color moving-image restoration method

Figure 1 shows a flow diagram of our recently proposed color moving-image restoration method [17]. Input signals to the

restoration method are heavily-degraded image sequences, mimicking color moving-image sequences acquired under the extremely-low-illumination condition.

*Poissonian-Gaussian color moving-image sequence*

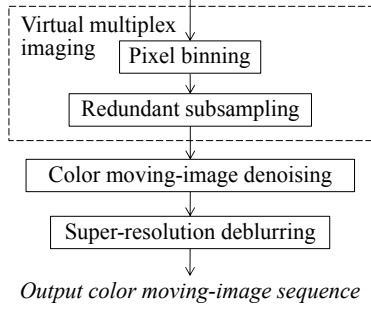


Fig. 1. Flow diagram of our recently proposed color moving-image restoration method [17].

### 2.1. Virtual multiplex imaging

In the flow diagram of Fig. 1, the restoration method firstly applies  $3 \times 3 \times 3$  spatiotemporal pixel-binning, a local small window of which is illustrated in Fig. 2, to the input image sequence. For a pixel of interest, a red-colored pixel in Fig. 2, the spatiotemporal pixel-binning sums up values of all 27 pixels inside a  $3 \times 3 \times 3$  local window surrounding the pixel of interest. Actually, in the restoration method, the spatiotemporal pixel-binning is constructed as the  $3 \times 3 \times 3$  simply-averaging filter.

The pixel binning was originally developed to increase sensitivity of an image sensor [19]. The pixel binning is a method to produce virtual observation values equivalent to those acquired by a virtual image-sensor with a larger-than-real pixel aperture. This paper extends the concept of the pixel binning, by combining it with the subsequent redundant subsampling, which means to simulate multiplex imaging achieved by virtual cameras with low spatiotemporal resolution and high sensitivity.

Secondly, the restoration method performs 3:1 3-D redundant subsampling whose structure is correspondent to the pixel binning. In the case of 3:1 subsampling in the 3-D space of  $(x, y, t)$ , there are 27 ( $= 3^3$ ) different subsampling patterns. Each subsampling pattern is specified by the 3-D coordinates  $(x_s, y_s, t_s)$  of its starting point, viz.  $(0, 0, 0), (0, 0, 1), \dots, (2, 2, 2)$ . The restoration method performs the 3:1 3-D subsampling with all the 27 different subsampling patterns, and it produces a set of 27 subsampled image sequences each of which is scaled down to one third in each dimension of the 3-D space. This paper refers to this type of subsampling as the redundant subsampling. In the subsequent color moving-image denoising stage, each of the 27 subsampled image sequences is separately processed with a color moving-image denoising method.

The serial application of the spatiotemporal pixel-binning and the 3-D redundant subsampling amounts to simulating multiplex imaging, achieved by virtual cameras with low spatiotemporal resolution and high sensitivity, which improves the signal-to-noise power ratio of the input image sequence and causes the probability distribution to approach the signal-dependent Gaussian distribution.

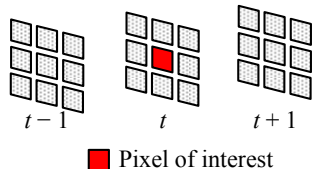


Fig. 2. Local window of the spatiotemporal pixel binning.

### 2.2. Color moving-image denoising

Thirdly, the restoration method applies a certain color moving-image denoising method, which shows high denoising performance for signal-dependent Gaussian noise, to each of the multiple subsampled sequences, thus to produce multiple denoised image sequences.

For denoising each of the 27 subsampled image sequences, this paper generally adopts either our previously proposed color moving-image denoising method, viz. the 3D-RDCT-CS (3-D Redundant DCT Color-Shrinkage) method [20], or the CVBM3D color moving-image denoising method [21], which is one of the state-of-the-art moving-image denoising methods.

The 3D-RDCT-CS method firstly applies the 3D-RDCT [20] to an input color moving-image sequence, and then processes each AC transform coefficient with the hard color-shrinkage [22], and finally converts the shrunk coefficients to the original space by the least-squares-type generalized inverse transform of the 3D-RDCT, thus to produce a denoised image sequence.

### 2.3. Super-resolution deblurring

Lastly, to remove image blurs caused by the pixel binning selectively, the restoration method performs super-resolution deblurring by integrating the set of the multiple denoised image sequences into a single image sequence with the spatiotemporal resolution identical to that of the input sequence, thus to produce an output image sequence.

This super-resolution deblurring problem is easy to solve, because the number of unknown variables is equal to that of available independent linear constraint equations and in addition to it all the degradation process in the virtual multiplex imaging is very simple and plain. However, we cannot expect that there exists a unique solution satisfying all the linear constraint equations simultaneously, and we need to seek a desirable solution that approximately satisfies all the simultaneous linear constraint equations and renders its regularization semi-norm, representing the inadequacy of a restored image, as low as possible. From this point of view, for the super-resolution deblurring, we adopt the total-variation (TV) semi-norm as the regularization semi-norm, and construct the restoration method as an iterative reconstruction algorithm that repeats the back-projection process [23] and the TV (Total-Variation) denoising process [24] alternately.

The classic back-projection method tends to amplify high-frequency components, and it often has an undesirable effect on noise visibility. To cope with this problem, the iterative reconstruction algorithm applies the TV denoising to the sequence updated by the immediately preceding back-projection step. As for the TV-denoising algorithm, this paper employs the 2-D ROF (Rudin-Osher-Fatemi) algorithm [24], and handles each frame of the sequence separately.

Formally speaking, the alternate iteration should be continued until convergence. However, actually the maximum number of iterations is set to  $N_{\max}$  in advance; when the iteration count arrives at  $N_{\max}$ , the iteration is stopped forcibly.

## 3. Experimental simulations

Our proposed restoration method is experimentally evaluated by computer simulations with a Poissonian-Gaussian test image sequence, artificially generated from the ITE standard image sequence, named ‘Intersection’, a certain image frame of which is shown in Fig. 3.



Fig. 3. Certain original image frame of the ITE standard color moving-image sequence, named ‘Intersection’.

### 3.1. Method of experimental simulations

Figure 4 shows how to generate a Poissonian-Gaussian test image sequence and how to conduct experimental simulations of restoration on the test image sequence.

In Fig. 4, its part enclosed with dotted lines corresponds to a flow diagram of generating the test image sequence. As shown in Fig. 4, firstly, the  $\gamma$ -correction is applied to a value of each pixel in an original image sequence, to convert an image-sequence’s signal to its light quantity  $a$ . Secondly, at each pixel of the image sequence, its light quantity  $a$  is divided by the light-limiting parameter  $D$ , thus to get a mean parameter  $\lambda$  of the Poisson distribution. Thirdly, at each pixel, a Poisson random number with the mean parameter  $\lambda$  is generated, a white Gaussian noise with zero mean and variance  $\sigma^2$  is added to it, and a Poissonian-Gaussian random number  $u$  is yielded. Lastly, for the normalization of signal’s intensity of  $u$ , each pixel’s value is multiplied by the light-limiting parameter  $D$ , thus to produce a Poissonian-Gaussian test image sequence  $r$ . In the experimental simulations, the light-limiting parameter  $D$  and the variance  $\sigma^2$  are set to 64 and 4, respectively, which is a parameter-setting realistic for the extremely-low-illumination imaging.

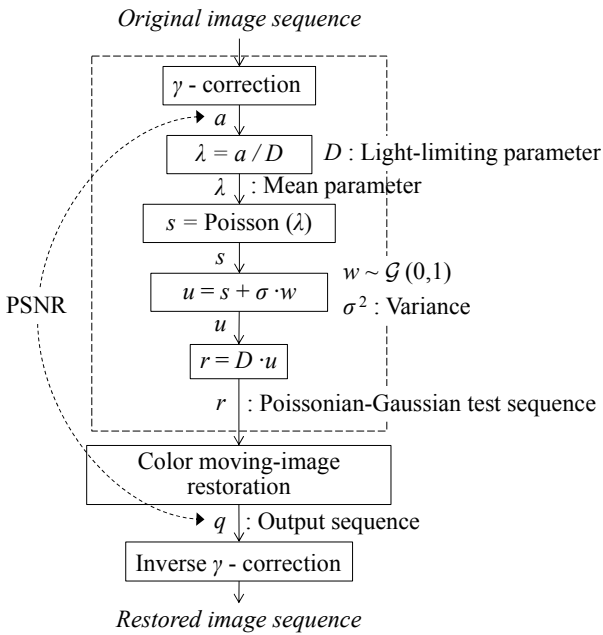


Fig. 4. Flow diagram of the experimental simulations.

Our proposed restoration method is applied to the Poissonian-Gaussian test sequence  $r$ , and then the inverse  $\gamma$ -correction is applied to the output image sequence  $q$ , thus to produce a finally-recovered image sequence that is actually displayed. To

evaluate restoration performance objectively, a peak signal-to-noise ratio, PSNR [dB], is calculated between the  $\gamma$ -corrected input image sequence  $a$  and the output image sequence  $q$  provided by our proposed restoration method.

For comparison, this paper evaluates restoration performance of two variant types of our proposed restoration method. The two variant types are as follows.

- 1) Variant A: The super-resolution deblurring stage is skipped, and instead each of the 27 denoised image sequences is magnified to three times in each dimension with the nearest neighbor interpolation method, and a recovered sequence is produced by averaging all the 27 magnified sequences.
- 2) Variant B: The two stages of the virtual multiplex imaging and the super-resolution deblurring are omitted; and hence a recovered sequence is simply provided by the denoising method.

In both the variant A and the variant B, our 3D-RDCT-CS denoising method [20] is employed as the denoising method.

### 3.2. Results of experimental simulations

Figure 5 shows PSNR’s of recovered image sequences versus the maximum number of iterations,  $N_{\max}$ , at the super-resolution deblurring stage. In Fig. 5, as  $N_{\max}$  is set to a higher value, the PSNR gradually improves to some extent. However, even if  $N_{\max}$  is set to a value higher than 20, the improvement in the PSNR is not significant and elevation of subjective picture-quality of the recovered sequence is very little. In the simulations,  $N_{\max}$  is fixed at 20.

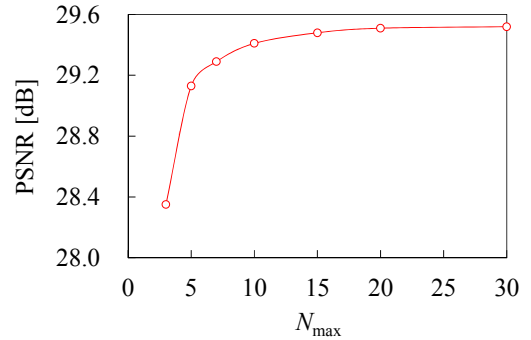


Fig. 5. PSNR’s of recovered image sequences versus the maximum number of iterations,  $N_{\max}$ , at the super-resolution deblurring stage.

Figure 6 shows PSNR’s of every frame in recovered image sequences versus the frame number  $k$ . In Fig. 6, PSNR’s provided by our proposed restoration method are compared with those provided by the Variant A, the Variant B, and the Mäkitalo-and-Foi’s restoration method with the generalized Anscombe transform [14] and the CVBM3D color moving-image denoising method [21], abbreviated to ‘the MF-GA method’ in the following. As for our proposed restoration method, as the color moving-moving image denoising method, either the 3D-RDCT-CS denoising method [20] or the CVBM3D denoising method [21] is applied. As shown in Fig. 6, the Variant A performs most poorly, and the Variant B outperforms the Variant A, which means that the introduction of the virtual multiplex imaging without the super-resolution deblurring results in the deterioration in restoration performance instead of improvement. Our proposed restoration method with the 3D-RDCT-CS denoising method performs best, and gives higher PSNR’s by 1 [dB] or more than the Variant B and the MF-GA method; the introduction of the virtual multiplex

imaging and the super-resolution deblurring together contributes to this superiority in restoration performance. As for the denoising method in our proposed restoration approach, the results of Fig. 6 show that the 3D-RDCT-CS denoising method is more suitable than the CVBM3D denoising method.

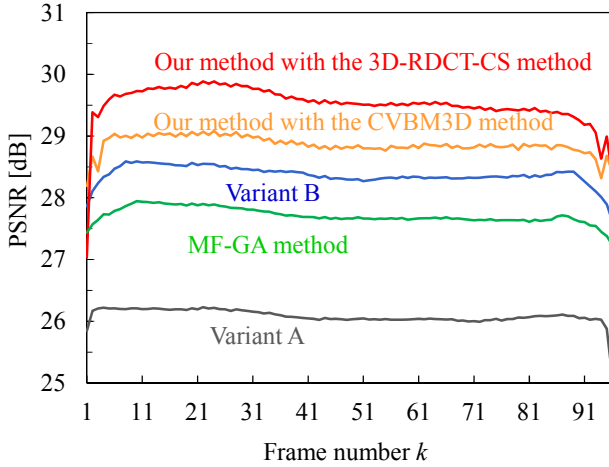


Fig. 6. PSNR's of every frame in recovered image sequences versus the frame number  $k$ .

Figure 7 compares portions of certain image frames of color moving-image sequences recovered by the four different restoration methods: our proposed restoration method, the Variant A, the Variant B, and the MF-GA method. The Poissonian-Gaussian test image of Fig. 7 (a) is produced by omitting the image-restoration processing from the flow diagram of Fig. 4. In the cases of Fig. 7 (c), (d), and (e), the 3D-RDCT-CS denoising method [20] is employed as the denoising method, but in the case of Fig. 7 (b) and (f) the CVBM3D denoising method [21] is employed as the denoising method.

As shown in Fig. 7 (b), the MF-GA method fails to restore objects' true colors and textures and it produces false color smears as a side effect. The MF-GA method does not necessarily perform well, because the generalized Anscombe transform does not function as properly as expected as the variance stabilization under the extremely-low-illumination photographing condition. The Variant B also produces false color smears; the Variant A restores objects' true colors, but reconstructs an image giving a blurry visual impression. On the other hand, our proposed restoration method succeeds in recovering a relatively-high-quality image, and reconstructs an image giving the sharpest visual impression. As shown in Fig. 7 (f), our proposed method with the CVBM3D denoising method restores a moving-image sequence giving a slightly sharper visual impression than our proposed method with the 3D-RDCT-CS denoising method, but fails in restoring fine image textures and objects' true colors correctly. On the other hand, as shown in Fig. 7 (e), our proposed method with the 3D-RDCT-CS denoising method succeeds in removing the image blurs caused by the pixel binning to a considerable extent and restoring objects' true colors correctly. However, roughly speaking, the comparison between Fig. 7 (e) and (f) suggests that our proposed restoration method visually achieves restoration performance almost at the same level, irrespective of a color moving-image denoising method actually employed at the denoising stage, as long as the employed denoising method shows a fairly efficient denoising performance for a noisy color moving-image sequence.



(a) Poissonian-Gaussian test image, 9.09 [dB]



(b) MF-GA method with the CVBM3D method [21], 27.71 [dB]



(c) Variant B with the 3D-RDCT-CS method [20], 28.37 [dB]



(d) Variant A with the 3D-RDCT-CS method [20], 26.08 [dB]



(e) Our method with the 3D-RDCT-CS method [20], 29.50 [dB]



(f) Our method with the CVBM3D method [21], 28.86 [dB]

Fig. 7. Recovered color moving-image sequences.

## 4. Conclusion

For the restoration of a Poissonian-Gaussian color moving-image sequence, this paper presents our recently proposed image restoration approach composed of the three consecutive stages: the virtual multiplex imaging, the color moving-image denoising, and the super-resolution deblurring. Experimental simulations demonstrate that the introduction of both the virtual multiplex imaging and the super-resolution deblurring into the restoration approach definitely contributes toward reconstructing a relatively-high-quality color moving-image sequence from a heavily-corrupted color moving-image sequence taken under the extremely-low-illumination photographing condition. As shown in this paper, the state-of-the-art highly-advanced image-restoration technique will be able to extend the potential of a solid-state image sensor further beyond its seemingly physical restriction.

## References

- [1] E. R. Fossum, "What to do with sub-diffraction-limit (SDL) pixels?—A proposal for a gigapixel digital film sensor (DFS)," *Proc IEEE Workshop CCDs Adv. Image Sensors*, pp. 214–217 (Sep. 2005).
- [2] J. Ma and E. R. Fossum, "Quanta image sensor jot with sub 0.3e- r.m.s. read noise and photon counting capability," *IEEE Electron Device Letters*, vol. 36, no. 9, pp. 926–928 (Sep. 2015).
- [3] J. Ma and E. R. Fossum, "A pump-gate jot device with high conversion gain for a quanta image sensor," *IEEE J. Electron Devices Soc.*, vol. 3, no. 2, pp. 73–77 (Mar. 2015).
- [4] F. Yang, Y. M. Lu, L. Sbaiz, and M. Vetterli, "Bits from photons: oversampled image acquisition using binary poisson statistics," *IEEE Trans. Image Process.*, vol. 21, no. 4, pp.1421–1436 (Apr. 2012).
- [5] S. H. Chan and Y. M. Lu, "Efficient image reconstruction for gigapixel quantum image sensors," *Proc IEEE Global Conf. on Signal and Information Processing (Global SIP 2014)*, pp. 312–316 (Dec 2014).
- [6] O. A. Elgendy and S. H. Chan, "Image reconstruction and threshold design for quanta image sensors," *Proc. of 2016 IEEE Int. Conf. on Image Processing (ICIP 2016)*, pp. 978–982 (Sept. 2016).
- [7] B. Zhang, J. M. Fadili, and J. -L. Starck, "Wavelet, ridgelets, and curvelets for Poisson noise removal," *IEEE Trans. Image Process.*, vol.17, no.7, pp.1093-1108 (July 2008).
- [8] H. Talbot, H. Phelippeau, M. Akil, and S. Bara, "Efficient Poisson denoising for photography," *Proc. 2009 IEEE Int. Conf. Image Process.*, pp.3881-3884 (Nov. 2009).
- [9] M. A. Figueiredo and J. M. Bioucas-Dias, "Restoration of Poissonian images using alternating direction optimization," *IEEE Trans. Image Process.*, vol. 19, no. 12, pp. 3133-3145 (Dec. 2010).
- [10] M. Mäkitalo and A. Foi, "A closed-form approximation of the exact unbiased inverse of the Anscombe variance-stabilizing transformation," *IEEE Trans. Image Process.*, vol.20, no.9, pp.2697-2698 (Sep. 2011).
- [11] K. Hirakawa and P. J. Wolfe, "Skellam shrinkage: wavelet-based intensity estimation for inhomogeneous Poisson data," *IEEE Trans. Inform. Theory*, vol.58, no.2, pp.1080-1093 (Feb. 2012).
- [12] R. Kobayashi, T. Komatsu, and T. Saito, "Restoration of Poissonian random images based on a statistical model," *Trans. IEICE*, vol. J96-D, no.9, pp.1993-1997 (Sept 2013).
- [13] X. Jin, Z. Xu, and K. Hirakawa, "Noise parameter estimation for Poisson corrupted images using variance stabilization transforms," *IEEE Trans. Image Process.*, vol.23, no.3, pp.1329-1339 (Mar. 2014).
- [14] M. Mäkitalo and A. Foi, "Optimal inversion of the generalized Anscombe transform for Poisson-Gaussian noise," *IEEE Trans. Image Process.*, vol.22, no.1, pp.91-103 (Jan. 2013).
- [15] Y. L. Montagner, E. D. Angelini, and J. -C. Olivo-Marin, "An unbiased risk estimator for image denoising in the presence of mixed Poisson-Gaussian noise," *IEEE Trans. Image Process.*, vol. 23, no.3, pp.1255-1268 (Mar. 2014).
- [16] E. Chouzenoux, A. Jezierska, J. -C. Pesquet, and H. Talbot, "A convex approach for image restoration with exact Poisson-Gaussian likelihood," *SIAM J. Imaging Sci.*, vol. 8, no.4, pp. 2662–2682 (Nov. 2015).
- [17] T. Komatsu, S. Kondou, and T. Saito, "Restoration of a Poissonian-Gaussian color moving-image sequence with virtual multiplex imaging and super-resolution deblurring," *Proc. of 2016 IEEE Int. Conf. on Image Processing (ICIP 2016)*, pp. 1963-1967 (Sept. 2016).
- [18] K. Dabov, A. Foi, and K. Egiazarian, "Image restoration by sparse 3D transform-domain collaborative filtering," *IEEE Trans. Image Process.*, vol.16, no.8, pp.2080-2095 (Aug. 2007).
- [19] Z. Zhou, B. Pain, and E. Fossum, "Frame-transfer CMOS active pixel sensor with pixel binning," *IEEE Trans. Electron. Dev.*, vol. 44, no.10, pp.1764-1768 (Oct. 1997).
- [20] S. Kondou, T. Komatsu, and T. Saito, "A note on a video denoising method with the redundant 3D-DCT," *Proc. 2014 IEICE Gen. Conf.*, D-11-53 (Mar. 2013).
- [21] K. Dabov, A. Foi, and K. Egiazarian, "Video denoising by sparse 3D transform-domain collaborative filtering," *Proc. 15th European Signal Process. Conf. (EUSIPCO 2007)*, pp.145-149 (Sep. 2007).
- [22] T. Saito, Y. Ueda, and T. Komatsu, "Color shrinkage for sparse coding of color images," *Proc. 18th European Signal Process. Conf. (EUSIPCO 2010)*, pp.1023-1027 (Aug. 2010).
- [23] H. Stark (Ed.), "Image recovery: theory and application," Academic Press, Inc. (1987).
- [24] L. I. Rudin, S. Osher, and E. Fatemi, "Nonlinear total variation based noise removal algorithms," *Physica D*, vol. 60, no.1-4, pp. 259-268 (Nov. 1992).